Polymer 49 (2008) 2595–2603

Contents lists available at ScienceDirect

Polymer

journal homepage: www.elsevier.com/locate/polymer

# Graft-type poly(*N*-isopropylacrylamide-*co*-acrylic acid) microgels exhibiting rapid thermo- and pH-responsive properties

Jie Zhang[a], Liang-Yin Chu[a,b,*], Chang-Jing Cheng[a], Dan-Feng Mi[a], Ming-Yu Zhou[a], Xiao-Jie Ju[a]

[a] *School of Chemical Engineering, Sichuan University, Chengdu, Sichuan, 610065, China*
[b] *Institute for Nanobiomedical Technology and Membrane Biology, State Key Laboratory of Biotherapy, Sichuan University, Chengdu, Sichuan 610065, China*

ARTICLE INFO

*Article history:*
Received 9 November 2007
Received in revised form 1 February 2008
Accepted 24 March 2008
Available online 29 March 2008

*Keywords:*
Graft copolymers
Microgels
Rapid response

## ABSTRACT

A novel graft-type poly(*N*-isopropylacrylamide-*co*-acrylic acid) (poly(NIPAM-*co*-AAc)) microgel with linear grafted poly(NIPAM-*co*-AAc) side chains was prepared by incorporating the dual stimuli-responsive chains into conventional copolymerized poly(NIPAM-*co*-AAc) backbones as side chains through a grafted modification of molecular structure. The grafted chains with unfettered ends can unfold and shrink freely in response to environmental stimuli. Due to the mobile nature and the tractive force of the grafted poly(NIPAM-*co*-AAc) side chains, the prepared microgels were verified to have a synchronously rapid thermo- and pH-response property. When the environmental temperature was increased suddenly from 25 °C to about 63 °C, the graft-type microgels in ultrapure water deswelled 95% by volume at best within 40 s but the normal-type microgels deswelled only 17% by volume within the same period. The analogous trends were observed in either alkaline or acid buffered solution. The graft-type microgels may thus be very promising for use in many applications in which rapid responses to dual environmental stimuli are required.

## 1. Introduction

Because of their unique volume phase-transition properties in response to environmental changes, stimuli-sensitive hydrogels have attracted much attention in the past 20 years [1–3]. These stimuli-sensitive "intelligent" hydrogels are considered to have potential for application in numerous fields, including drug delivery, chemical separations, chemical sensors, enzyme and cell immobilization [4–11]. Poly(*N*-isopropylacrylamide) (PNIPAM) is a widely investigated thermo-sensitive polymer that undergoes a volume phase transition around the lower critical solution temperature (LCST, approximately 32 °C) [12,13]. Early studies have mainly been limited to the macroscopic hydrogels that need a long time to reach the swelling equilibrium. However, for a lot of potential applications, a fast response is necessary for their practical usage. Tanaka et al. have demonstrated that the responsive time is approximately in proportion to the square of a linear dimension of the gel [14,15]. Moreover, the size of the gel needs to be small enough to exert effects in many particular regions, especially the drug delivery systems. Thereupon, microgels with much faster volume change than macroscopic hydrogels with the same chemical structure, have recently attracted increasing attention and many significant results have been obtained [16–18].

However, to broaden the functions of microgels in the aforementioned applications, it is desirable to incorporate other functional groups within the gel matrix. Along these lines, microgels with temperature- and pH-sensitivity have been commonly investigated in more recent works, because both parameters are important environmental factors in biomedical and other systems [19–25]. Usually, pH-ionizable monomer with carboxylic acid groups is incorporated into PNIPAM-based gel networks by randomly copolymerizing to provide a pH-sensitive property for the thermo-responsive gels [26–28].

Nevertheless, the randomly introduced ionic groups will also result in an adverse effect. Impregnating microgels with them would reduce or even eliminate the thermo-sensitivity due to the increase in the hydrophilicity and the break in the continuous thermo-sensitive isopropylamide pendant groups of PNIPAM [29–31]. In some cases, the strong electrostatic repulsion will even smear out the temperature-induced transition [23]. These effects greatly limit the potential application of such hydrogels. For instance, an acting actuator requires an instantaneous feedback after receiving signals.

In order to achieve improved dual stimuli-sensitive microgels with much faster response properties using conventional synthesis techniques, we evolved a novel strategy through a grafted

---

* Corresponding author. School of Chemical Engineering, Sichuan University, Chengdu, Sichuan, 610065, China. Tel.: +86 28 8546 0682; fax: +86 28 8540 4976.
*E-mail address:* chuly@scu.edu.cn (L.-Y. Chu).

0032-3861/$ – see front matter © 2008 Elsevier Ltd. All rights reserved.
doi:10.1016/j.polymer.2008.03.040

modification of molecular structure which had been put forward by Chen and Hoffman [32] and Yoshida et al. [33]. This technique has been developed in many aspects [34–41]. Based on a fixed total content of sensitive units that was same in normal copolymerizing method, this strategy modified their locations in gel structure only. Utilizing this methodology, we have synthesized a macroscopic hydrogel with rapid thermo- and pH-responsive phase-transition rate [42]. Unlike introducing the single thermo-sensitive PNIPAM grafted chains into hydrogel networks in our previous work [42], we prepared a dual thermo- and pH-sensitive macromonomer as the grafted chain with freely mobile ends in this study for the first time, and then incorporated them into the dual thermo- and pH-sensitive polymer backbone networks simply via free radical copolymerization. The novel microgel has potential for application in variety of fields, such as new drug carriers, and sensors. The effects of the novel chemical structure on the swelling and deswelling properties of microgels were investigated systematically by changing the environmental temperature and pH conditions.

## 2. Experimental section

### 2.1. Materials

*N*-Isopropylacrylamide (NIPAM; Kohjin Co.) was recrystallized from a mixture of acetone and *n*-hexane. Acrylic acid (AAc; Tianjin Bodi Chemical Engineering Co., Ltd.) was purified by vacuum distillation at 40 °C and 10 mm Hg. Tetrahydrofuran (THF; Chongqing Chuandong Chemical Engineering Co., Ltd.), 2-hydroxyethanethiol (HESH; Sanland-chem International Inc.), benzoyl peroxide (BPO; Tianjin Jingxing Chemical Reagents), diethyl ether (Tianjin 1st Chemical Reagents), acetone (Tianjin 1st Chemical Reagents), acryloyl chloride (Haimen Beisite Jingxi Chemical Engineering Co., Ltd.), chloroform (Tianjin Bodi Chemical Engineering Co., Ltd.), *N*,*N*′-methylene-bis-acrylamide (BIS; Chengdu Kelong Chemical Reagents), *N*,*N*,*N*′,*N*′-tetramethylethylenediamine (TEMED; Shanghai Qianjin Nongchang Reagents), ammonium peroxide (APS; Shanghai Chemical Reagents), and polyglycerol polyricinoleate (PGPR 90; Danisco Co., Ltd, Denmark) were used as received. Kerosene (Chengdu Shudu Chemicals) was filtrated before use. Fresh ultrapure water from a Milli-Q Plus water purification system (Millipore) was used throughout this work.

### 2.2. Synthesis of poly(NIPAM-co-AAc) macromonomer

A poly(NIPAM-*co*-AAc) macromonomer with a terminal hydroxyl end group poly(NIPAM-*co*-AAc)-OH was prepared by radical telomerization of the NIPAM monomer and the AAc monomer using HESH as a chain transfer agent (Fig. 1). NIPAM (6.78 g, 0.06 mol), AAc (1.03 mL, 0.015 mol), HESH (0.105 mL, 1.5 mmol), and BPO (0.0363 g, 0.15 mmol) were dissolved in THF (25 mL). The monomer solution was degassed by a freeze-thaw cycle and sealed in vacuum. Polymerization was carried by heating the reaction at 70 °C for 12 h. To precipitate poly(NIPAM-*co*-AAc)–OH, the reactant was poured into diethyl ether. Poly(NIPAM-*co*-AAc)–OH was collected by filtration and was purified by repeated precipitation in diethyl ether from acetone. The polymer was isolated by freeze-drying from aqueous solution. The purified poly(NIPAM-*co*-AAc)–OH was dissolved in chloroform, and acryloyl chloride (excess) was instilled, and the reaction was stirred at 40 °C for 2 h under nitrogen atmosphere, and finally poly(NIPAM-*co*-AAc) macromonomer was isolated using the procedure described above for poly(NIPAM-*co*-AAc)–OH.

### 2.3. Characterization of macromonomer

$^1$H NMR and FT-IR spectra were recorded on a Bruker-400 spectroscopy using $D_2O$ as the solvent and on a NICOLET-560 spectroscopy, respectively. The molecular weight of semi-telechelic poly(NIPAM-*co*-AAc)-OH was estimated by gel permeation chromatography (GPC, Waters 515 pump with Waters 2410 refractive-index detector) using THF as the mobile phase and polystyrene as the standard. Molar component ratio of NIPAM and AAc in the macromonomer was determined to be 79.84 mol% and 20.16 mol%, respectively, by $^1$H NMR spectroscopy.

### 2.4. Preparation of poly(NIPAM-co-AAc) microgels

Poly(NIPAM-*co*-AAc) microgels were prepared by inverse suspension polymerization using kerosene as the continuous phase and PGPR as oil-soluble surfactant. Certain NIPAM, AAc, poly(NIPAM-*co*-AAc) macromonomer and 0.015 g BIS were dissolved in 5 mL ultrapure water containing 10 mg APS, and the mixture was bubbled with nitrogen for 15 min to remove dissolved oxygen. This solution was immediately poured into 80 mL kerosene containing 3.368 g PGPR, which was previously purged with nitrogen. The reaction mixture was stirred at 1450 rpm under nitrogen atmosphere for 25 min. After formation of relatively uniform aqueous emulsion droplets in continuous phase was confirmed, 50 μL of TEMED was added to the continuous phase to initiate polymerization. The polymerization was allowed to proceed for 2.5 h at 25 °C (Fig. 2). After polymerization, the microgels were separated from the oil phase and were washed with mixture of abluent and ultrapure water once and then washed with ultrapure water five

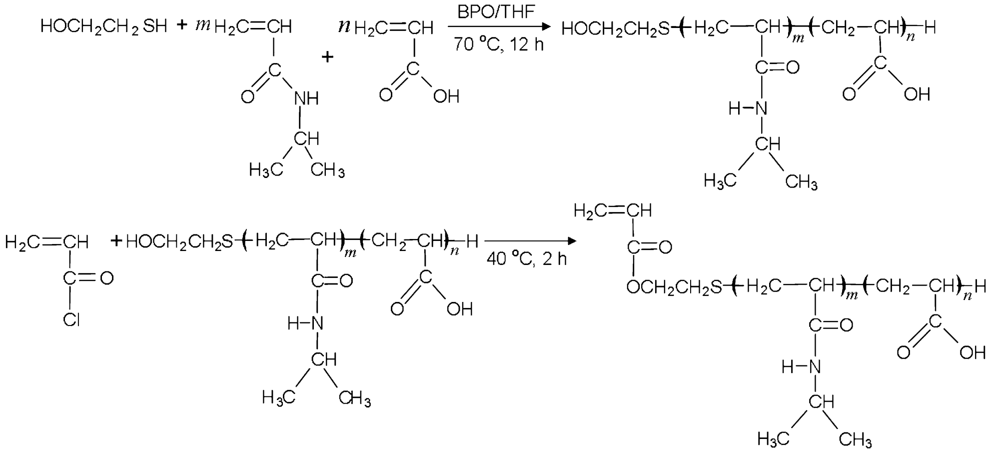

Fig. 1. Preparation of poly(NIPAM-*co*-AAc) macromonomer.

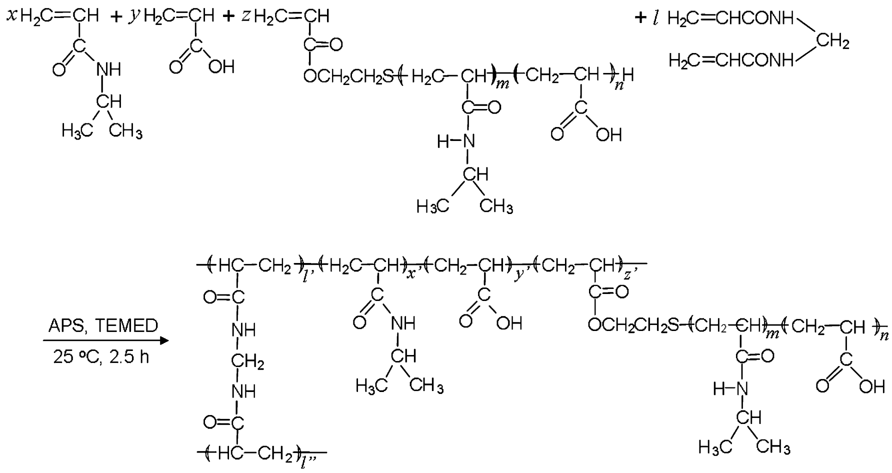

Fig. 2. Synthetic scheme for the preparation of the poly(NIPAM-*co*-AAc) microgel with dual sensitive grafted chains.

**Table 1**
Feed compositions for the preparation of poly(NIPAM-*co*-AAc) microgels

| Component | Sample code | | |
|---|---|---|---|
| | PNA[a] | PNAm-1[a,b] | PNAm-2[a,b] |
| NIPAM monomer (mg) | 528.2 | 431.0 | 397.7 |
| AAc monomer (μL) | 35 | 20 | 15 |
| PNA macromonomer (mg) | 0 | 114.0 | 151.5 |

*Note*: cross-linker BIS = 15 mg; accelerator TEMED = 50 μL; APS initiator = 10 mg; solution (ultrapure water) = 5 mL; emulsifier PGPR = 3.368 g; and continuous phase kerosene = 80 mL.

[a] The total molar ratio of NIPAM/AAc in the whole sensitive monomers was kept to about 9:1.

[b] The molar ratio of NIPAM/AAc in macromonomer was about 4:1 according to the result of $^1$H NMR spectroscopy.

times. The feed compositions of monomers and other chemicals are listed in Table 1.

### 2.5. Equilibrium swelling/deswelling degree of microgels

Some microgels were placed in a glass cell filled with ultrapure water, and the temperature was controlled in the range from 25 °C to 60 °C by a thermostatic stage system (TS62, Instec, USA). Microgels were observed using an optical microscope (BX61, Olympus Co., Ltd., Japan), and the pictures were recorded by a CCD camera connected to the microscope. Diameters of about 100 of microgels at each temperature were analyzed to calculate the mean diameter, $D_m$. The mean equilibrium swelling/deswelling diameters of the microgel samples in buffered solutions (the ionic strength was adjusted to 0.1 M beforehand) were measured at 25 °C.

### 2.6. Deswelling kinetics of microgels

The deswelling kinetics of the microgels were measured under different conditions. Microgels were allowed to swell in 0.1 M buffer (pH 7.4 and pH 2.0) at 25 °C for 48 h, and the buffer was refreshed every day. Selected swollen microgels were placed in a glass cell filled with the same buffer and observed under the microscope. The samples were allowed to reach equilibrium in ultrapure water or buffered solutions at 25 °C and were then transferred to the thermostatic stage system where the temperature was held at 63 °C. In order to measure the deswelling kinetics of them in the condition that pH and temperature are changed, the microgels that had been pre-equilibrated in pH 7.4 buffered solutions at 25 °C were placed in a glass cell and then the solutions were removed. After being added pH 2.0 solution in, the cells were immediately transferred to the thermostatic stage system where

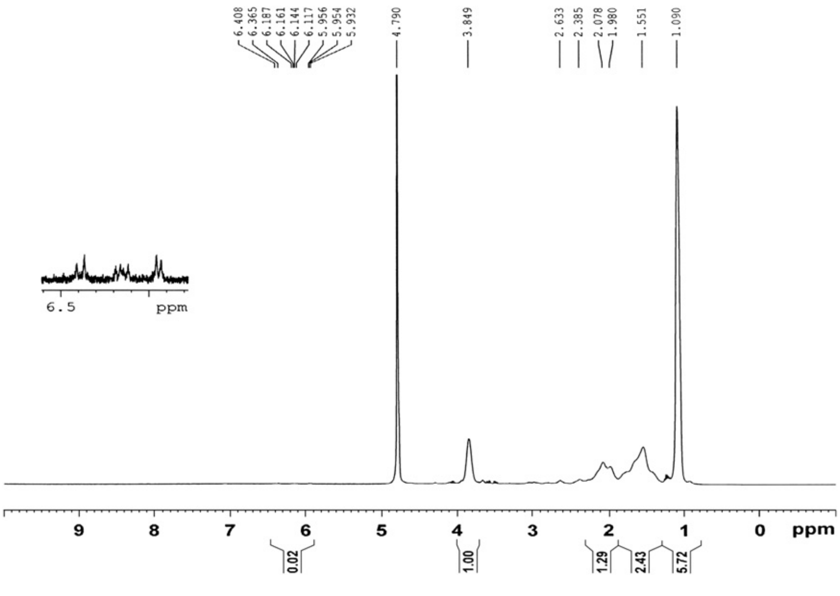

Fig. 3. $^1$H NMR spectrum of the poly(NIPAM-*co*-AAc) macromonomer.

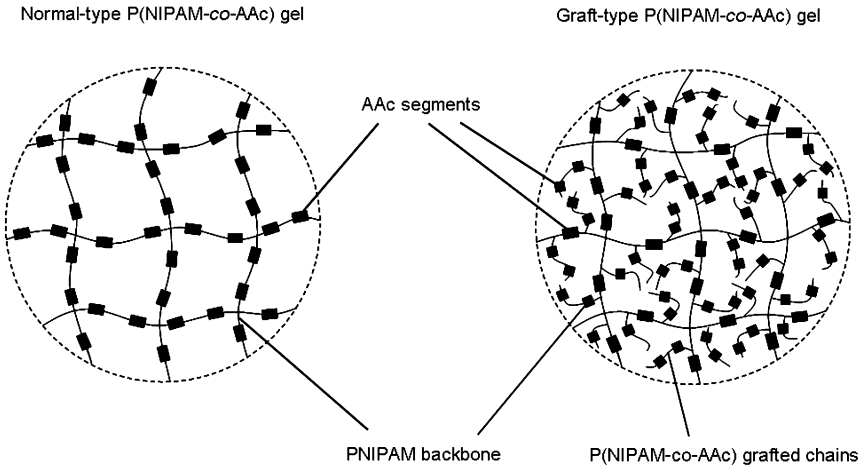

**Fig. 4.** Schematic illustration of the microstructures of normal-type and graft-type poly(NIPAM-*co*-AAc) microgels.

the temperature was held at 63 °C. At regular time intervals, the pictures of samples were recorded and diameters of the same passel of microgels were measured to calculate the mean diameter. The ratio of mean volume, $V_t/V_0$, was calculated from $D_m$, where $V_t$ was the mean volume of microgels at time $t$ and $V_0$ was the mean volume at the beginning of the deswelling.

## 3. Results and discussion

### 3.1. Synthesis and characterization of poly(NIPAM-co-AAc) macromonomer

The poly(NIPAM-*co*-AAc) macromonomer was prepared by radical telomerization of NIPAM and AAc monomers using HESH as a chain transfer agent. A spectrum of the macromonomer obtained with $^1$H NMR spectroscopy measurements exhibited peaks at 1.1 ppm (–$CH_3$) and 3.9 ppm (–CH–), while two broad peaks at 1.6 and 2.0 ppm due to methylene proton and methyne proton on the main chains were observed. Significantly, the peaks of vinyl proton at 5.9–6.5 ppm were detected, indicating that a polymerizable end group was introduced into the hydroxyl semi-telechelic poly(NIPAM-*co*-AAc) (Fig. 3). FT-IR spectroscopy measurements were carried out. As expected, two characteristic peaks of NIPAM at 1643.9 cm$^{-1}$ (amide I) and at 1549.0 cm$^{-1}$ (amide II) appeared and the peak consistent with carboxyl groups at 1716.1 cm$^{-1}$ was detected, indicating that AAc was introduced into the macromonomer. The weight-average and number-average molecular weights of the macromonomer were determined to be 3195 Da and 2215 Da, respectively, by gel permeation chromatography.

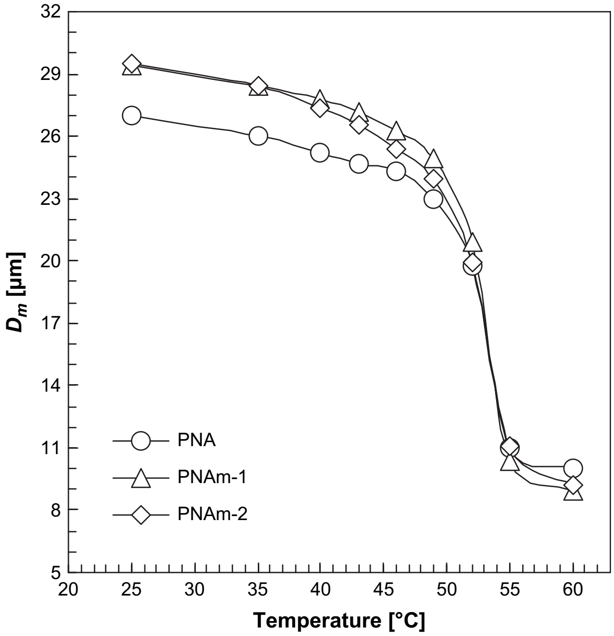

**Fig. 5.** Temperature dependence of the equilibrium mean diameters of normal-type and graft-type poly(NIPAM-*co*-AAc) microgels in water in the temperature range from 25 to 60 °C.

### 3.2. Preparation of poly(NIPAM-co-AAc) microgels

Graft-type poly(NIPAM-*co*-AAc) microgel was prepared by free radical copolymerization of poly(NIPAM-*co*-AAc) macromonomer with NIPAM and AAc in the presence of BIS as a cross-linker. Normal-type microgel is also prepared without adding macromonomer, as illustrated in Fig. 2. The backbone networks were made up of the NIPAM and the AAc components, and the linear poly(NIPAM-*co*-AAc) polymers served as the freely mobile chains and were grafted onto the backbone by fixing one end structurally. Within the microgel, the grafted chains had freely mobile ends, distinct from the typical network structure in which both ends of chains are cross-linked and relatively immobile. Schematic structures of normal-type and graft-type microgels are provided in

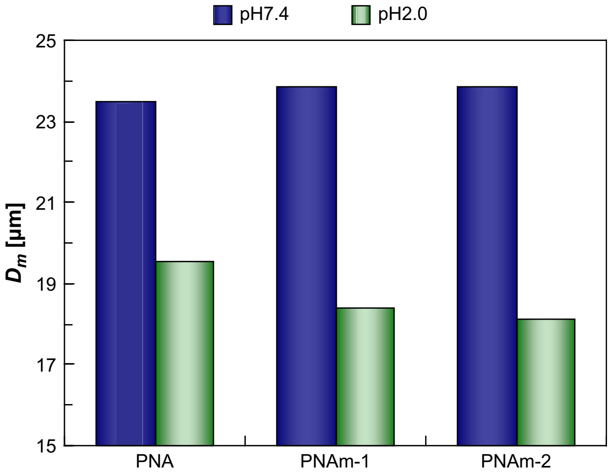

**Fig. 6.** Equilibrium mean diameters of normal-type and graft-type poly(NIPAM-*co*-AAc) microgels in buffer solutions at pH 7.4 and pH 2.0, respectively, at room temperature (25 °C).

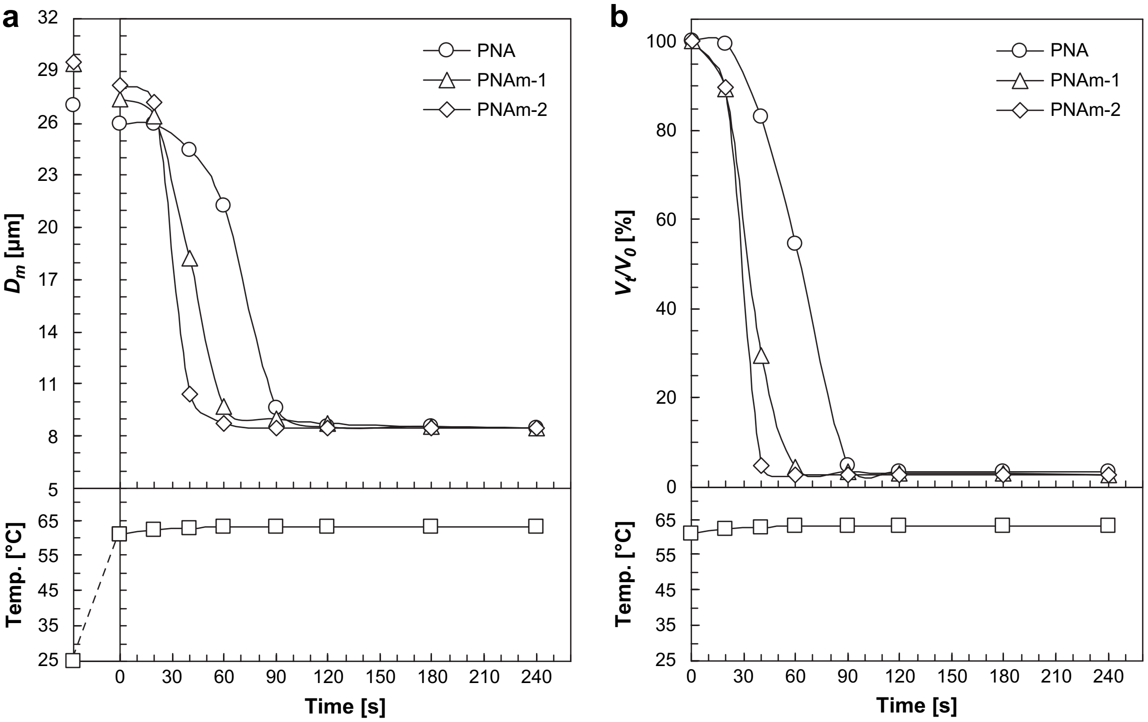

**Fig. 7.** Deswelling kinetics of microgels at about 63 °C measured from an equilibrium swelling condition at 25 °C in ultrapure water.

Fig. 4. As listed in Table 1, the graft-type microgels constructed with different contents of macromonomer and AAc are designated as PNAm-1 and PNAm-2, respectively; normal-type microgels without grafted chains are designated as PNA. The total weight of NIPAM, AAc and poly(NIPAM-*co*-AAc) macromonomer in PNAm-1, PNAm-2 and PNA microgels was kept constant. Furthermore, the respective ratio of thermo-sensitive and pH-sensitive components in each kind of microgels was ensured to be constant.

### 3.3. *Temperature dependence of the swelling/deswelling degree of microgels in ultrapure water*

Equilibrium swelling/deswelling degrees of graft-type and normal-type poly(NIPAM-*co*-AAc) microgels in ultrapure water are plotted as a function of temperature in Fig. 5. The introduction of hydrophilic AAc into the polymer framework caused the LCSTs of microgels to increase, as a higher temperature was needed to drive the disruption of strengthened hydrogen bonds. Nevertheless, the phase-transition behaviors indicated that the graft-type microgels showed the same phase-transition temperature (~53 °C) as that of the normal-type microgels. That means the AAc content in every type of microgels was kept constant and the recipe to prepare both PNA and PNAm microgels ensured that the quantity of thermo-sensitive components as well as pH-sensitive components was constant. PNAm microgels exhibit higher swelling degree in swollen state below the LCST and lower deswelling degree in collapsed state above the LCST than PNA microgels. As the grafted chains are structurally separated from the backbone cross-linked network, stronger hydration may be possible. This chain expansion is considered to result in increased hydration in PNAm microgels. Controlling the amount of grafted chains can regulate the equilibrium swelling properties of microgels.

### 3.4. *Equilibrium swelling/deswelling degree of microgels in pH buffers*

Fig. 6 shows the equilibrium swelling/deswelling degrees of graft-type and normal-type poly(NIPAM-*co*-AAc) microgels in pH buffers at 25 °C. Due to the effects of ionic strength, the equilibrium swelling degrees of the microgels in pH buffers were universally smaller than those in ultrapure water [43]. With increasing pH, more and more carboxylic groups (–COOH) within the microgels are deprotonated to the anionic $–COO^-$ form so that the internal electrostatic repulsion within the microgels is enhanced [44,45]. On the other hand, there was a probably intrachain hydrogen-bonding association between the NIPAM and the AAc units at low surrounding pH [46]. Thus, all of microgels were swollen in pH 7.4 buffer and were shrunk in pH 2.0 buffer. Compared with PNA microgels, PNAm ones were a little more swollen in pH 7.4 buffer, but more shrunk in pH 2.0 buffer to a certain extent. That is, the incorporation of the grafted chains into microgel makes the pH-sensitive swelling/deswelling degree improved. Comparing with PNAm-1 microgels, the PNAm-2 microgels with more side chains showed more prominent phenomenon. On the condition at pH 7.4, the hydration of mobile grafted chains were stronger and the electrostatic repulsive forces operating between the charged carboxyl groups of acrylic acid made the grafted chains more extended which towed the whole networks to a more swollen state. On the other hand at pH 2.0, the grafted chains that shrank due to the electrostatic repulsive force vanished between the uncharged carboxyl groups that made the hydration of them decreased and then towed the whole networks to a more collapsed state. Obviously, the pH-sensitivity brought from AAc on grafted chains was the decisive effect to the response of microgels to pH changes, but the effect of AAc on rigid main chains was relatively puny.

### 3.5. *Deswelling kinetics of microgels in ultrapure water*

Fig. 7 shows the deswelling kinetics of PNA and PNAm microgels after a temperature jump from the equilibrium state in ultrapure water at 25 °C to above the LCST (at 63 °C). The microgels swelled at 25 °C and the volume was ranked in order of the number of grafted chains. The normal-type microgels shrunk slowly in response to temperature changes with a nearly changeless stage in the beginning 20 s and reached the minimal shrinkage state after 120 s. In

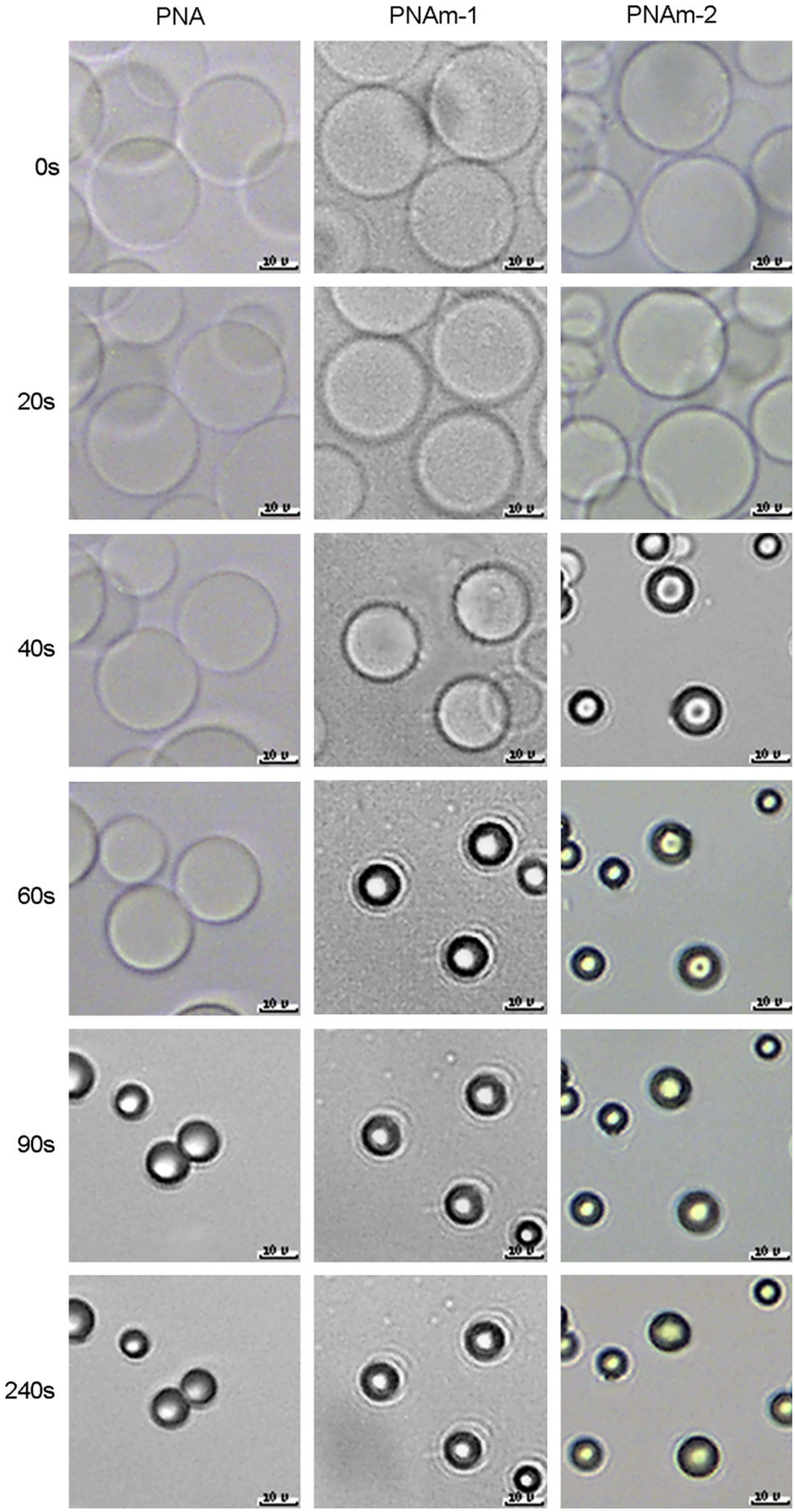

**Fig. 8.** Photographs of the deswelling process of normal-type (PNA) and graft-type microgels (PNAm-1 and PNAm-2) undergoing shrinking at about 63 °C after being suddenly heated from an equilibrium condition at 25 °C. Scale bar is 10 μm.

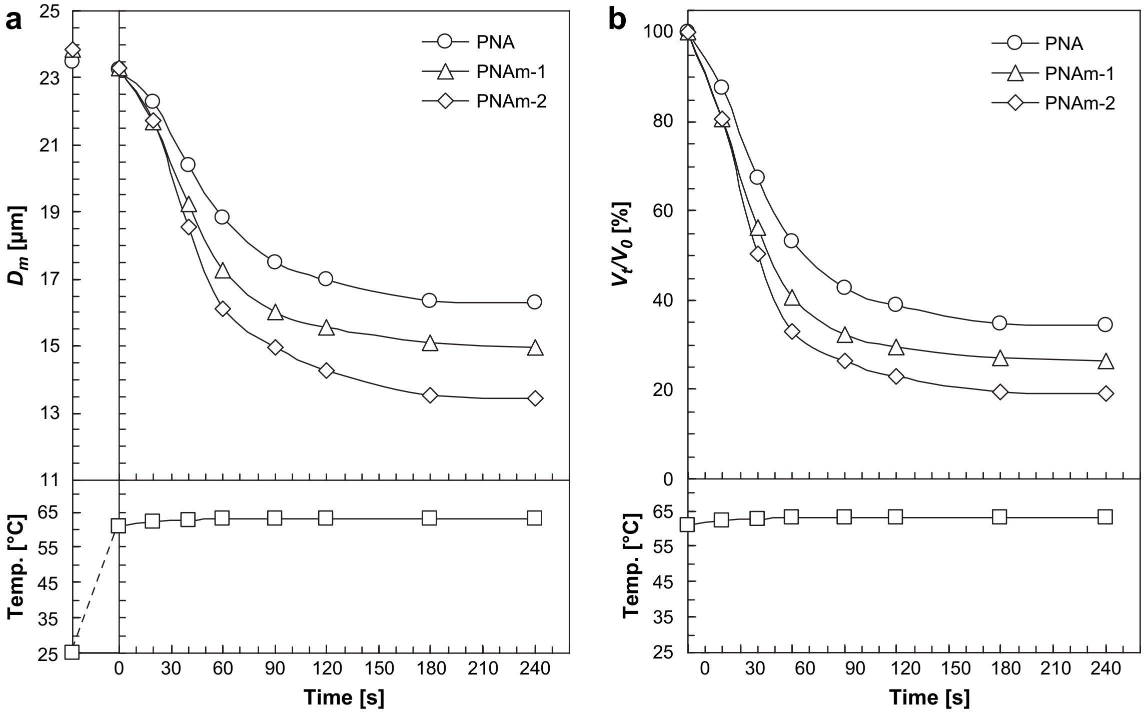

**Fig. 9.** Deswelling kinetics of microgels at about 63 °C measured from an equilibrium swelling condition at 25 °C in buffered solution with pH = 7.4.

contrast, shrinking of the graft-type microgels was much rapid with a sharp deswelling and reached the minimal shrinkage state after about 60 s, and the quick response was ranked in the order of the content of macromonomer. For instance, at the point of 40 s, PNAm-1 and PNAm-2 microgels have deswelled about 70% and 95% by volume, respectively; but the normal-type microgels have deswelled only about 17% by volume. On the other hand, the mean diameters of all microgels were almost the same after 120 s.

The actual shrinking processes of PNA, PNAm-1 and PNAm-2 microgels are demonstrated in the series of photographs in Fig. 8. Comparing with that of the normal-type PNA microgels with rigid frame architecture, such rapid shrinkage of the graft-type PNAm microgels is due to the immediate dehydration of the NIPAM moieties on freely mobile grafted chains in the gel matrixes, followed by subsequent hydrophobic interactions between dehydrated grafted chains preceding shrinkage of the whole network and resulting in rapid expulsion of water from the gel matrix [24]. On the other hand, when the NIPAM units aggregated at higher temperatures, the incorporated hydrophilic AAc segments which brought counterforce to hydrophobic aggregation forces maintained hydration and also restricted the shrinkage of microgels synchronously. Even though the two forces are contradictory, the hydrophobic forces overwhelmed the hydrophilic forces in the matrixes. Nevertheless, there were the same contents of AAc in each type of microgels as forenamed but their distribution was different. The hydrophilic AAc segments located on the main chains of the normal-type microgels restricted the shrinkage of microgels, which resulted in that PNA microgels shrunk slowly to a certain extent. For PNAm microgels, the AAc moieties were not only located on the main chains, but also distributed on the grafted chains with freely mobile ends, therefore the hydrophilic effects might be extremely delicate compared with the strong hydrophobic aggregation effects. In short, the resistances to shrinkage were smaller in PNAm microgels than that in PNA microgels. Clearly, greater hydrophobic aggregation forces were engendered within PNAm microgels having a greater number of branched grafted chains according to the difference between the PNAm-1 and PNAm-2 microgels. Nevertheless, all microgels showed almost the same sizes at the equilibrium shrunken state, because they were small enough to squeeze out the interior water in short order.

### 3.6. Deswelling kinetics of microgels in pH buffers

In order to probe into the dual stimuli-sensitivity of the microgels, the deswelling kinetics of the microgels were studied under the conditions with both temperature and pH adjusted. In the experiments, the microgels had been pre-equilibrated in pH 7.4 buffered solutions at 25 °C before measurement, and then the environmental temperature was suddenly increased to 63 °C. Similar phenomena to those described in Section 3.5 are observed in the deswelling process, as illustrated in Fig. 9. Again, the PNAm-1 and PNAm-2 microgels with grafted chains possessing freely mobile ends in the polymeric networks showed more rapid deswelling than normal-type PNA microgels. On the other hand, the volume change degrees of all microgels were not as large as those in ultrapure water. According to their pH-sensitive nature, the polymer chains expanded because of electrostatic repulsions among the charged carboxyl groups of AAc in alkaline solution. Upon an external temperature increase, the freely mobile grafted chains would collapse and the backbone of networks would also shrink due to their NIPAM component at the same time. For PNA microgels, the electrostatic repulsions of the AAc moieties on the backbone would impair the shrinking forces, saying nothing of the absence of strong collapses of grafted chains. In PNAm microgels, where the AAc moieties were partly on the main chains and the others were on the grafted chains with freely mobile ends, the repulsive forces would be too small to counteract with shrinking forces brought from grafted chains and the backbone of networks together. The more grafted chains the microgels have, the larger shrinking force the microgels create, and as a result the more rapid deswelling the microgels exhibit. Besides the hydrophilic effects of the AAc moieties, just as those in microgels during the deswelling process in

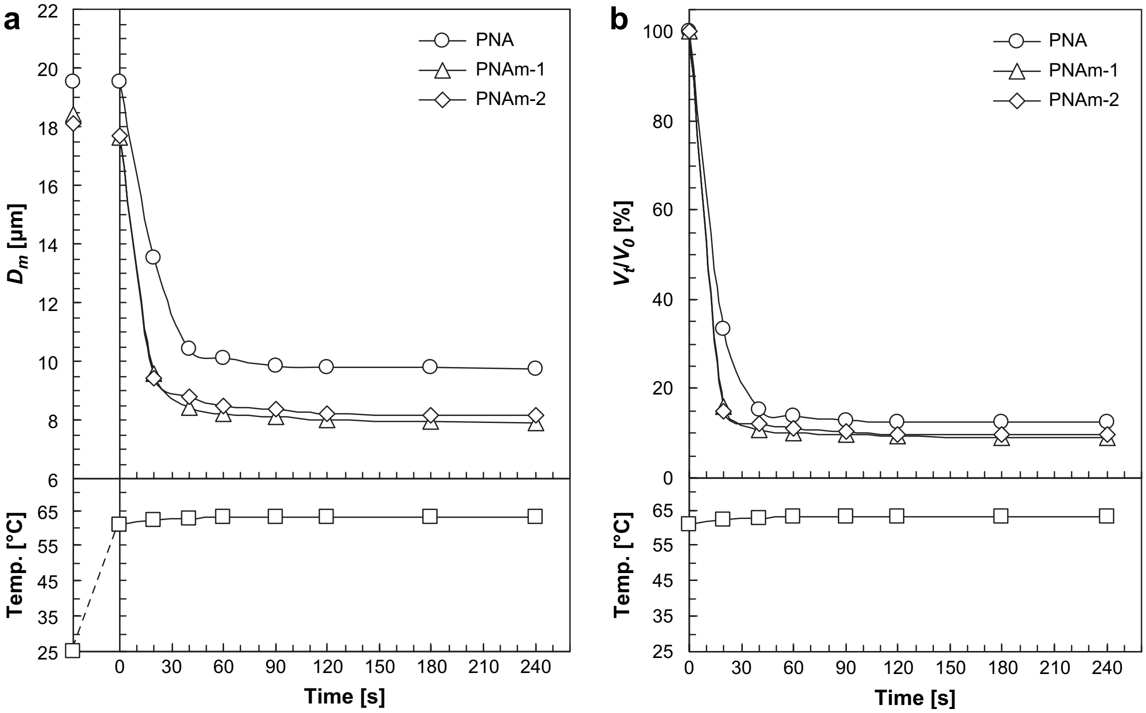

**Fig. 10.** Deswelling kinetics of microgels at about 63 °C measured from an equilibrium swelling condition at 25 °C in buffered solution with pH = 2.0.

ultrapure water, there were still the electrostatic repulsions of the AAc moieties in all microgels under this condition. These two effects restrained the shrinkage of microgels to a greater extent; as a result, the deswelling degrees of microgels were smaller than those in ultrapure water.

Fig. 10 shows the shrinking kinetics of microgels in a pH 2.0 buffered solution after a temperature jump from 25 to 63 °C. It can be clearly seen that the shrinking rates of all the microgels were much larger than those described above. They have achieved the shrunken equilibrium in about 40 s. However, the PNAm microgels deswelled more quickly than the PNA microgels. One interesting trend was that the PNAm-2 microgels deswelled slightly faster than the PNAm-1 microgels in the beginning but became slightly slower to reach a new equilibrium, and the other was that the last mean diameters of the PNA microgels were slightly larger than that in ultrapure water. Upon experiencing an external temperature increase to above the LCST, for PNAm microgels, the immediate response to temperature occurred, which would cause a much

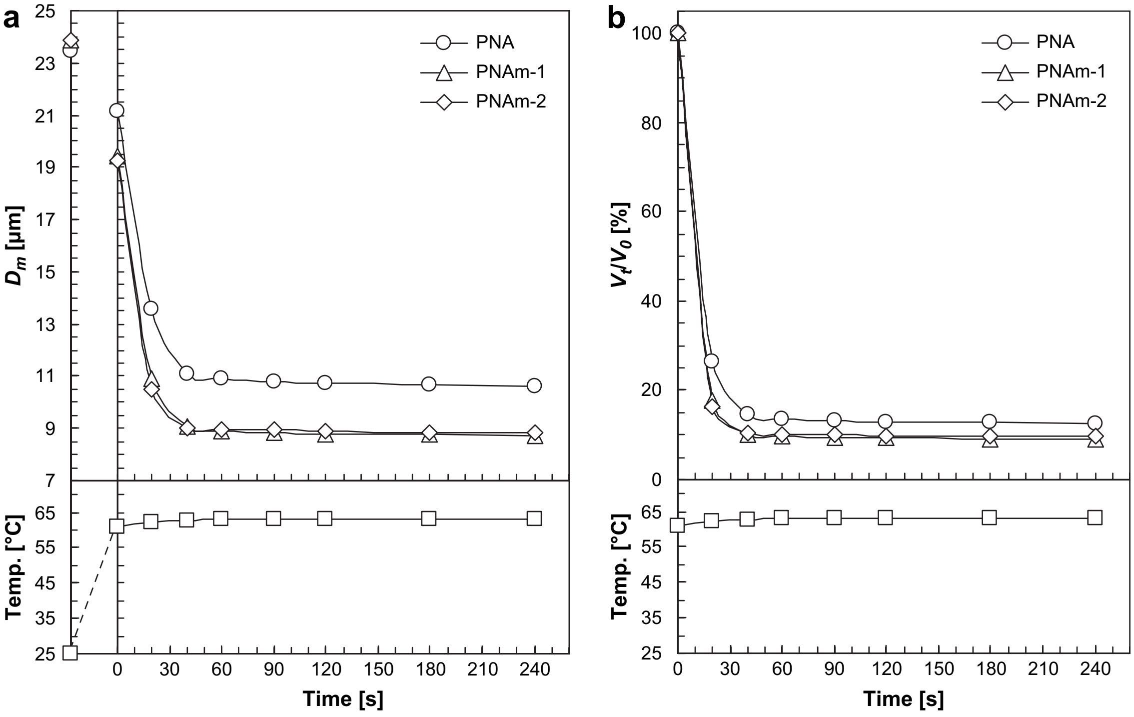

**Fig. 11.** Deswelling kinetics of microgels in buffer at pH 2.0 and 63 °C measured from an equilibrium swelling condition in buffer at pH 7.4 and 25 °C.

faster shrinkage in the lack of counteraction of electrostatic repulsions. Likewise, the AAc moieties and the intrachain hydrogen-bonding association would produce contracting layers in an acidic solution, but the forces would be milder than those caused by the temperature response. Thus, the rapid shrinking would destroy the layers for packing solution, leading to a rapid release of solution from the microgels' interior in a short time. Subsequently, when the hydrophobic aggregation reached an utmost, the deswelling rate of the microgels with more grafted chains slowed down because of weakened thermo-sensitive effects and less contents of the NIPAM moieties on the main chains according to the recipe. The PNA microgels shrunk slower than PNAm microgels in the early phase of the deswelling process because of a lack of grafted chains, and then more aqueous solution might be preserved by the not-well-destroyed skin layers due to the higher density of AAc in the backbone networks. Thus, they have greater sizes than that in ultrapure water at last.

Investigations on microgels in response to dual temperature and pH changes were also carried out. Fig. 11 shows the time course of deswelling for microgels undergoing shrinking in pH 2.0 buffer at 63 °C after an abrupt change from pH 7.4 and 25 °C. The results were almost the same as the trends in the foregoing condition. These microgels were so small that the pH buffered solution could soak into them in a short time. Thus, the actual environment was similar to the condition at pH 2.0 after changing. It is obvious to note that these microgels have shrunk quite a bit in a few seconds after the pH transfer before heating from 25 °C, especially those microgels with grafted chains possessing freely mobile ends inside the polymeric networks. That is, the deswelling rate of the microgels responding to single pH change was also rapid. The grafted chains did enhance the pH-responsibility of the dual stimuli-sensitive microgels, just as they enhanced the temperature responsibility.

## 4. Conclusions

Graft-type poly(NIPAM-*co*-AAc) microgels with dual stimuli-responsive grafted chains were successfully prepared. The results showed that the temperature dependence of the swelling degree of the microgels in ultrapure water is dominated by the quantity of thermo-sensitive and pH-sensitive components, regardless of its location in the microgel. The grafted chains in the polymeric networks inside the microgels responding to both temperature and pH stimuli could unfold and shrink freely so as to drive the whole framework to swelling and deswelling. The molecular mobility of polymers was improved and rapid responses to temperature and pH was obtained as a result of the introduction of grafted chains with freely mobile ends into the polymer networks. The equilibrium properties and rate of deswelling of microgels were controlled by the content of the grafted chains. Comparing with the normal-type microgels, rapid deswelling dynamics of graft-type microgels were observed in ultrapure water as well as in pH buffered solutions whether it was alkaline or acid. From aforementioned results, it is obvious that the AAc moieties on the grafts would not restrain the thermo-responsibility of microgels unlike the actions of those on the backbone networks, and they would enhance the pH-responsibility markedly. Based on the strategy presented in this study, it is possible to develop new multi stimuli-sensitive microgels with improved responses to environment stimuli.

## Acknowledgments

The National Natural Science Foundation of China (20674054), the Key Project of the Ministry of Education of China (106131) and the Specialized Research Fund for the Doctoral Program of Higher Education by the Ministry of Education of China (20040610042) are acknowledged for supporting this research. The authors are grateful to the Kohjin Co., Ltd., Japan, for kindly supplying the *N*-isopropylacrylamide.

## References

[1] Hirokawa Y, Tanaka TJ. Chem Phys 1984;81:6379.
[2] Tanaka T, Sato E, Hirokawa Y, Hirotsu S. Phys Rev Lett 1985;55:2455.
[3] Holtz JH, Asher SA. Nature 1997;389:829.
[4] Sauzedde F, Pichot C. Colloid Polym Sci 1999;277:846.
[5] Hoffman AS. Adv Drug Deliv Rev 2002;54:3.
[6] Kawaguchi H, Fujimoto K. Bioseparation 1998;7:253.
[7] Kasgoz H, Orbay M. Polymer 2003;44:1785.
[8] Suzuki H. J Intel Mat Syst Str 2006;17:1091.
[9] Kwon IC, Bae YH, Kim SW. Nature 1991;354:291.
[10] Ogawa Y, Ogawa K, Kokufuta E. Langmuir 2001;17:2670.
[11] Ogawa K, Wang BL, Kokufuta E. Langmuir 2001;17:4704.
[12] Pelton RH, Pelton HM, Morfesis A, Rowell RL. Langmuir 1989;5:816.
[13] Tanaka Y, Kagami Y, Matsuda A, Osada Y. Macromolecules 1995;28:2574.
[14] Matsuo ES, Tanaka T. J Chem Phys 1988;89:1695.
[15] Li Y, Tanaka T. J Chem Phys 1989;90:5161.
[16] Zhang QS, Zha LS, Ma JH, Liang BR. Macromol Rapid Commun 2007;28:116.
[17] Suarez IJ, Fernandez NA, Marquez M. J Phys Chem B 2006;110:25729.
[18] Matsumura Y, Iwai K. Polymer 2005;46:10027.
[19] Tan BH, Tam KC. Polymer 2007;48:6589.
[20] Li X, Zuo J, Guo YL, Yuan XH. Macromolecules 2004;37:10042.
[21] Hoare T, Pelton R. Macromolecules 2004;37:2544.
[22] Kuckling D, Vo CD, Wohlrab SE. Langmuir 2002;18:4263.
[23] Jones CD, Lyon LA. Macromolecules 2000;33:8301.
[24] Pich A, Tessier A, Boyko V, Lu Y, Alder HJ. Macromolecules 2006;39:7701.
[25] Zhou S, Chu B. J Phys Chem B 1998;102:1364.
[26] Serizawa T, Wakita K, Akashi M. Macromolecules 2002;35:10.
[27] Shibayama M, Fujikawa Y, Nomura S. Macromolecules 1996;29:6535.
[28] Chen H, Hsieh YL. J Polym Sci Part A Polym Chem 2004;42:6331.
[29] Beltran S, Baker JP, Hooper HH, Blanch HW, Prausnitz JM. Macromolecules 1991;24:549.
[30] Feil H, Bae YH, Feijan J, Kim SW. Macromolecules 1993;26:2496.
[31] Ebara M, Aoyagi T, Sakai K, Okano T. Macromolecules 2000;33:8312.
[32] Chen GH, Hoffman AS. Nature 1995;373:49.
[33] Yoshida R, Uchida K, Kaneko Y, Sakai K, Kikuchi A, Sakurai Y, et al. Nature 1995;374:240.
[34] Zhang CL, Feng LF, Gu XP, Hoppe S, Hu GH. Polymer 2007;48:5940.
[35] Zhang XH, Shen Z, Li L, Lu GL, Gu LN, Huang XY. Polymer 2007;48:5507.
[36] Peng D, Zhang XH, Feng C, Lu GL, Zhang S, Huang XY. Polymer 2007;48:5250.
[37] Peng D, Zhang XH, Huang XY. Polymer 2006;47:6072.
[38] Neugebauer D. Polymer 2007;48:4966.
[39] Li ZY, Li PP, Huang JL. Polymer 2006;47:5791.
[40] Kutsevol N, Guenet JM, Melnik N, Sarazin D, Rochas C. Polymer 2006;47:2061.
[41] Ballauff M, Lu Y. Polymer 2007;48:1815.
[42] Zhang J, Chu LY, Li YK, Lee YM. Polymer 2007;48:1718.
[43] Jeria OM, Pizarro GDC, Marambio OG, Huerta M, Geckeler KE. J Appl Polym Sci 2006;100:1735.
[44] Liu Y, Velada JL, Huglin MB. Polymer 1999;40:4299.
[45] Wang Y, Liu ZM, Han BX, Dong ZX, Wang JQ, Sun DH, et al. Polymer 2004;45:855.
[46] Bokias G, Staikos G, Iliopoulos I. Polymer 2000;41:7399.